H.C. Henninger, J.D. Biggs
Optimal Under-Actuated Kinematic Motion Planning on the Epsilon-Group
Automatica, Vol. 90, 2018, p. 185-195
doi:10.1016/j.automatica.2017.12.049

Optimal under-actuated kinematic motion planning on the ϵ-group *

Helen C. Henninger[a], James D. Biggs[a],

[a] *Dipartimento di Scienze e Tecnologie Aerospaziale, Politecnico di Milano, Via La Masa 34 - 20156 Milano, Italy*

Abstract

A global motion planning method is described based on the solution of minimum energy-type curves on the frame bundle of connected surfaces of arbitrary constant cross sectional curvature ϵ. Applying the geometric framing of Pontryagin's principle gives rise to necessary conditions for optimality in the form of a boundary value problem. This arbitrary dimensional boundary value problem is solved using a numerical shooting method derived from a general Lax pair solution. The paper then specializes to the 3-dimensional case where the Lax pair equations are integrable. A semi-analytic method for matching the boundary conditions is proposed by using the analytic form of the extremal solutions and a closed form solution for the exponential map. This semi-analytical approach has the advantage that an analytic description of the control accelerations can be derived and enables actuator constraints to be incorporated via time reparametrization. The method is applied to two examples in space mechanics: the attitude control of a spacecraft with two reaction wheels and the spacecraft docking problem.

Key words: parametric optimization; control of vehicles; analytic design; motion planning; non-holonomic distributions

1 Introduction

This paper addresses the motion planning problem on the frame bundle and isometry group of m-dimensional simply connected surfaces of constant cross sectional curvature ϵ. The motion planner considered here deals with the case where ϵ is arbitrary with frame bundle, coined here, the ϵ-group G_ϵ. While according to the Killing-Hopf theorem, any complete connected Riemann space M^m, $m \geq 2$ of constant curvature ϵ has a universal cover $\mathbb{S}^m$, $\mathbb{H}^m$ or $\mathbb{E}^m$ and so the value of ϵ is usually set to 1, 0 or -1, we consider $\epsilon \in [-1, 0) \cup (0, 1]$ so that $\epsilon = 0$ can be considered only as a limiting case. This is useful in that for $\epsilon \neq 0$ the trace form is non-degenerate and our optimal control problem reduces to solving an identity derived from a Lax pair form. Moreover, a simple iterative map can be developed from this identity to numerically solve for the optimal solution $g \in \mathsf{G}_\epsilon$. In the case $\epsilon = 0$ no such Lax pair form exists due to the fact that it has a degenerate bi-linear trace form, but its solution can be considered in the limit.

The structure-preserving numerical method for solving optimal trajectores in this paper can be applied to arbitrary dimensions and for arbitrary curvature of the underlying space form (approximately optimal in the case $\epsilon = 0$ where we approximate it by a very small number in part of the numerical integration). In addition, the paper specializes to the completely integrable 3-D case where the extremal curves can be solved explicitly in terms of elliptic functions. Furthermore, the exponential map used to solve the boundary conditions is solved in closed-form for arbitrary ϵ. This leads us to a novel semi-analytic formulation for solving this class of optimal control problems on 3-D Lie groups for arbitrary ϵ. Moreover, in the integrable case the velocities and acceleration components can be derived from the analytically defined extremal curves and as such time-parameterization can be used to ensure dynamic feasibility of the kinematically feasibile solution.

As we consider m-dimensional Riemann spaces, the isometry group G_ϵ will correspond to the groups $\mathsf{SO}(m+1)$ (in the case $\epsilon = 1$), $\mathsf{SE}(m)$ (in the case $\epsilon = 0$) and $\mathsf{SO}(m, 1)$ (in the case $\epsilon = -1$). The dimension of G_ϵ is then $n = \frac{m(m+1)}{2}$. This paper initially considers systems whose configuration space $g \in \mathsf{G}_\epsilon$

*This paper was not presented at any IFAC meeting. Corresponding author H. C. Henninger. Tel. +39 3420270338.

Email Addresses: helenclare.henninger@polimi.it (Helen C. Henninger), jamesdouglas.biggs@polimi.it (James D. Biggs)

satisfies the following differential constraint

$$\begin{cases} \dot{g} & = g(\sum_{i=1}^{n} v_i A_i) \\ g(0) & = g_0 \quad \text{and} \quad g(t_f) = g_d. \end{cases} \tag{1}$$

The vector $[v_1, v_2, ..., v_n]^\top \in \mathbb{R}^n$ are continuous functions, $g \in \mathsf{G}_\epsilon$, and $A_1, ..., A_n$ is the basis of the ϵ-Lie algebra $\mathfrak{g}_\epsilon$.

There are a plethora of applications that can be modeled by (1). For example, the kinematics of various autonomous systems such as the attitude kinematics ($\epsilon = 1$, $n = 3$) of spacecraft [1–3], including those with velocity constraints [4] and those underactuated in control [5,6]. Systems such as wheeled robots, robotic grippers and slender underwater vehicles that exhibit a sliding-type constraint ($\epsilon = 0, n = 2$ or $n = 3$) [7–14] and in wider fields such as switched electrical networks [15], problems of quantum control [16] and planning curvature- and torsion-constrained 3D printed implants for facilitating radiation therapy [17]. Various methods have been developed to tackle the motion planning problem of left-invariant (respectively right) systems defined on matrix Lie groups of the form (1) where it is necessary to match the boundary condition $g(0) = g_0$ and $g(T) = g_T$. For example, the works [18] and [13] introduce the idea of solving non-holonomic motion planning problems by expressing the control analytically in terms of either elliptic functions [18] or sinusoids [13]. The parameters of these analytic control functions must then be computed to match the boundary conditions imposed on the motion planning problem. While the method we construct in this paper considers systems with non-holonomic constraints, for the purposes of controls these systems are treated as kinematic systems, i.e., the velocities are assumed to be directly controlled or equivalently the dynamics of the system can be perfectly canceled with the control. The distinction between these systems and dynamic non-holonomic systems is detailed in [31]. In [3], the author solves the necessary conditions for optimality using Pontryagin's principle and suggests using a standard numerical shooting method to solve for the boundary conditions via numerical integration. The paper [19] applies classical averaging theory; they produce sinusoidal controls that solve this motion planning problem with $O(\epsilon^p)$ accuracy in general, and exactly if the Lie algebra is nilpotent. The projection to the group is determined in local coordinates using the Wei-Norman product of exponentials representation and the Magnus single exponential representation. The paper [20] solves the problem for semi-simple and compact Lie groups via a continuation method. The restriction to a compact group is crucial to their handling, since the continuation method requires that the Wazewski equation must have a global solution. [21] proposes a general strategy for solving (1)-(19) by making use of an extended system, which comprises the original system plus higher-order Lie brackets of the system vector fields. The control which is determined by such a system provides an exact solution of the original problem if the given system is nilpotent or for the class of systems they classify as "feedback nilpotentizable", and for all other systems the solutions are approximate. The thesis [33] analyses the sub-Riemannian optimal control problems on $\mathsf{SO}(3)$ using a variational approach, while Brockett [34] and Jurdjevic [23] use the Pontryagin maximum principle. The work [32] analyzes the Hamiltonian structure of kinematic optimal control problems, particularly the sub-Riemannian optimal control problems on compact semi-simple Lie groups and gives a Lax pair form defining the necessary conditions for optimality for the special case where G_ϵ is the frame bundle of a Riemannian symmetric space; in this paper, G_ϵ is semi-simple and compact only in the case $\epsilon > 0$.

The general approach in this paper is to focus on a class of optimal solutions to the motion planning problem. Moreover, in addition to considering matching the boundary conditions the following quadratic cost is imposed

$$\mathcal{J} = \int_0^{t_f} \sum_{i=1}^{s} c_i v_i(t)^2 dt \tag{2}$$

where $s \leq n$ the time t_f is a fixed variable and $c_i > 0$ are constant scalar weights. Integrability of the extremal equations for an optimal control problem of this type has been detailed in [31]. Minimizing the cost (2) leads us to solve the system (1) as an optimal control problem, using the geometric framing of Pontryagin's maximum principle. However, the boundary conditions are not contained in the cost function and to match them specific values of the initial conditions of the extremal curves have to be computed. In this paper we derive an identity from the general Lax Pair solution that arises from this optimal control problem on Lie groups and use it to construct an iterative approach to solve the motion planning problem for prescribed boundary conditions. The approach has the advantages over previous methods as (i) it generalizes to a large class of n-dimensional systems with a left-invariant differential constraint defined on the frame bundles of spaces of arbitrary constant cross sectional curvature (ii) It does not require any analytical approximation methods such as averaging (iii) The curve $g(t)$ on the group is a global, co-ordinate-free solution. This means that the method avoids singularities and the un-winding problem that can be encountered when parameterizing the group (iv) the derived numerical shooting and integration method used for matching the boundary conditions preserves the first integral and the structure of the group.

The last section of the paper specializes to the completely integrable 3-D case for arbitrary ϵ. For the case where the optimal control problem lifts to a quadratic Hamiltonian a general solution to the extremal curves are explicitly solved in terms of Jacobi elliptic functions. Furthermore, a closed-form solution of the exponential map is derived which allows the construction of a semi-analytical shooting method. Due to the semi-analytical nature of

this case the required velocities,accelerations and controls can also be constructed analytically. The integrable cases, therefore, lend themselves to the possibility of time-paramaterization which can be used to ensure dynamic feasibility in practical problems. To this end the method is applied to two problems in space mechanics 1) the slewing of an underactuated spacecraft using only two reaction wheels and 2) a spacecraft docking problem where the spacecraft can only thrust in the forward and backwards directions of the body-fixed frame and it must rotate to point the thrusters in the required direction in inertial space.

2 Optimal trajectories of minimum-energy type on the ϵ-group

This section presents background to the geometric framing of Pontryagin's principle for the m-dimensional ϵ-group and some well-known properties of G_ϵ and its Lie algebra $\mathfrak{g}_\epsilon$ (§§2.1) as well as the form of the Lax pair equations for the n-dimensional case. A novel identity is constructed expressing the extremal curves on the Lie algebra $\mathfrak{g}_\epsilon$ in terms of the curve $g(t)$ which holds for all ϵ values ($\epsilon = 0$ is approached as a limiting case as $\epsilon \to 0$). This identity is then used to construct a simple iterative method alonside a first-order Lie symplectic Euler scheme to determine the initial extremals that are required to match the boundary conditions on the group.

2.1 Background

Here we review some known facts of optimal control on matrix Lie groups and facts about the ϵ-Lie algebra and fix notation. References used are [22–25, 31, 32].

Given the matrix $g \in \mathsf{G}_\epsilon$, and defining the $m+1 \times m+1$ matrix $J_\epsilon = \mathsf{diag}(1, \cdots, 1, \frac{1}{\epsilon})$, then for all integer ϵ,

1. $gJ_\epsilon g^\top = J_\epsilon$
2. $\det(g) = 1$.

Note that in the case $\epsilon = 1$, $\mathfrak{g}_1 = \mathfrak{so}(m+1)$, $\mathfrak{g}_{-1} = \mathfrak{so}(m,1)$ and $\mathfrak{g}_0 = \mathfrak{se}(m)$, the Lie algebras of the Special Orthogonal Group, Lorenz group and Special Euclidean Group, respectively.

For all values of ϵ, $\mathfrak{g}_\epsilon$ can be written as a direct sum $\mathfrak{g}_\epsilon = \mathfrak{p} \oplus \mathfrak{k}$, where in the case $\epsilon \neq 0$, this direct sum is a Cartan decomposition, i.e. the subalgebras $\mathfrak{p}$ and $\mathfrak{k}$ have the relations $[\mathfrak{p},\mathfrak{p}] \subseteq \mathfrak{k}$, $[\mathfrak{p},\mathfrak{k}] = \mathfrak{p}$ and $[\mathfrak{k},\mathfrak{k}] \subseteq \mathfrak{k}$. In the case $\epsilon = 0$, $[\mathfrak{p},\mathfrak{p}] = 0$ and the properties of the Cartan decomposition are lost.

For $\epsilon \neq 0$, the bilinear form

$$\kappa(A,B) = -\frac{1}{2}\mathrm{tr}(A\,B), \quad A, B \in \mathfrak{g}_\epsilon \tag{3}$$

is nondegenerate. Let $E_1, E_2, ..., E_m$ denote the standard basis for $\mathfrak{p}$ such that

$$a_1E_1 + ... + a_nE_m = \begin{bmatrix} 0 & \cdots & 0 & a_1 \\ \vdots & \vdots & \vdots & \vdots \\ 0 & \cdots & 0 & a_m \\ -\epsilon a_1 & \cdots & -\epsilon a_m & 0 \end{bmatrix}$$

and let $p_1, p_2, ..., p_m$ denote the coordinate of a point p in $\mathfrak{p}^*$ relative to the dual basis $E_1^*, E_2^*, ..., E_m^*$.
For each $p \in \mathfrak{p}^*$, let h^ϵ in $\mathfrak{g}_\epsilon$ be defined via the relation

$$p(A) = \kappa(h^\epsilon, A) \quad \text{for all } A \in \mathfrak{g}_\epsilon.$$

We denote $h_i = p(A_i)$ for any $p \in \mathfrak{g}_\epsilon^*$. It follows that

$$h^\epsilon = \begin{bmatrix} 0 & \cdots & 0 & \frac{1}{\epsilon}h_1 \\ \vdots & \vdots & \vdots & \vdots \\ 0 & \cdots & 0 & \frac{1}{\epsilon}h_m \\ -h_1 & \cdots & -h_m & 0 \end{bmatrix}.$$

The basis $A_1, A_2, ..., A_n$ of $\mathfrak{g}_\epsilon$ is chosen, such that $E_i = A_i$ for $i = 1, 2, ..., m$ and $\mathfrak{k} = \{A_{m+1}, ..., A_n\}$ (in the case $n = 3$ this corresponds to the basis (19)).

Given an element A of $\mathfrak{g}_\epsilon$ in the case $\epsilon = 0$, $A = A_p + A_k$ where $A_p \in \mathfrak{p}$, $A_k \in \mathfrak{k}$, a natural quadratic form can be defined:

$$\langle A, B\rangle_0 = \widehat{A}_p \cdot \widehat{B}_p + \langle A_k, B_k\rangle \tag{4}$$

where the map $\widehat{\ }\ : \mathfrak{p} \to \mathbb{R}^n$ denotes the hat map

$$\begin{bmatrix} 0 & \cdots & 0 & a_1 \\ \vdots & \vdots & \vdots & \vdots \\ 0 & \cdots & 0 & a_m \\ 0 & \cdots & 0 & 0 \end{bmatrix}\widehat{\ } = \begin{bmatrix} a_1 \\ \vdots \\ a_m \end{bmatrix}.$$

For $a, b \in \mathbb{R}^n$, $a = [a_1, \cdots, a_m]^\top$, $b = [b_1, \cdots, b_m]^\top$, the product $a \wedge b$ denotes the $m \times m$ antisymmetric matrix such that

$$(a \wedge b)(x) = (a \cdot x)b - (b \cdot x)a \quad \text{for all} \quad x \text{ in } \mathbb{R}^m. \tag{5}$$

Since using the nondegenerate form $\langle \cdot, \cdot \rangle_0$ in the case $\epsilon = 0$, $\mathfrak{g}_\epsilon^*$ may also be identified with $\mathfrak{g}_\epsilon$, and therefore in what follows all functions on $\mathfrak{g}_\epsilon^*$ will be mapped to $\mathfrak{g}_\epsilon$ for $\epsilon \in [0, 1]$.

The Pontryagin Maximum Principle [26] is a necessary condition for optimality which is most naturally expressed in the language of the geometry of the cotangent bundle $T^*\mathsf{G}_\epsilon$ of G_ϵ. The cotangent bundle $T^*\mathsf{G}_\epsilon$ can be trivialized (from the left) such that $T^*\mathsf{G}_\epsilon = \mathsf{G}_\epsilon \times \mathfrak{g}_\epsilon^*$, where $\mathfrak{g}_\epsilon^*$ is the dual space of the Lie algebra $\mathfrak{g}_\epsilon$ [23]. The Pontryagin maximum principle associates to (1)-(2) an optimal Hamiltonian function H on $T^*\mathsf{G}_\epsilon = \mathsf{G}_\epsilon \times \mathfrak{g}_\epsilon^*$. Using

the nondegenerate forms (3) and (4) $\mathfrak{g}_\epsilon^*$ will be identified with $\mathfrak{g}_\epsilon$ for all $\epsilon \in [0,1]$ and so in our case the Hamiltonian function is a function on $\mathsf{G}_\epsilon \times \mathfrak{g}_\epsilon$.

An optimal trajectory $g(\cdot) : [0, t_f] \to \mathsf{G}_\epsilon$ is a projection of an integral curve $(g(\cdot), h(\cdot))$ of the time-varying Hamiltonian vector field $\overrightarrow{H}$ that satisfies the boundary conditions given in (1)-(2). This is called the projection "downstairs", and $h(\cdot)$ is the extremal curve, or the projection "upstairs" of $(g(\cdot), h(\cdot))$. The projection downstairs satisfies the differential equation

$$g^{-1}(t)\left(\frac{dg}{dt}\right) = dH$$

where $dH = \sum_{i=1}^{m} \frac{\partial H}{\partial h_i} A_i + \sum_{j=m+1}^{n} \frac{\partial H}{\partial h_j} A_j$ and we denote $\Omega_\epsilon = \sum_{i=1}^{m} \frac{\partial H}{\partial h_i} A_i \in \mathfrak{p}$ and $\Omega_k = \sum_{j=m+1}^{n} \frac{\partial H}{\partial h_j} A_j \in \mathfrak{k}$.

Here a proposition is presented which gives the differential equation in Lax pair form satisfied by the projection upstairs on $\mathfrak{g}_\epsilon$.

Proposition 1. *[25] For optimal control problems of the form* (1)-(2) *in the case $\epsilon \neq 0$, the extremal is the solution of the following differential equations:*

$$\begin{aligned} \dot{g} &= g(t)dH && (6)\\ \dot{h}^k &= [h^k, \Omega_k] + \frac{1}{\epsilon}[\epsilon h^\epsilon, \Omega_\epsilon] && (7)\\ \epsilon\dot{h}_\epsilon &= [\epsilon h^\epsilon, \Omega_k] + \epsilon[h^k, \Omega_\epsilon] && (8) \end{aligned}$$

where $h \in \mathfrak{g}_\epsilon$, $h = h^k + h^\epsilon$, $h^k = h_{m+1}A_{m+1} + ... + h_n A_n \in \mathfrak{k}$. In the case $\epsilon = 0$, the equations (7)-(8) *are given by*

$$\begin{aligned} \dot{h}^k &= [h^k, \Omega_k] + \widehat{L}_p \wedge \widehat{\Omega}_0 && (9)\\ \dot{h}^p &= [h^p, \Omega_k] && (10) \end{aligned}$$

where $h^p = \lim_{\epsilon\to} \epsilon h^\epsilon$. The equations (9)-(10) *follow from equations* (7)-(8) *as $\epsilon \to 0$.*

We prove a new result which will be needed for solving the extremal equations in the non-integrable case in such a way that $\epsilon \in [-1, 1]$ can be dealt with in an inclusive fashion.

Theorem 1. *Given the solution curve upstairs, $h(t) = h^k(t) + h^\epsilon(t)$, on $\mathfrak{g}_\epsilon$ for $\epsilon \neq 0$, it satisfies the equation*

$$g(t)(\epsilon h^k(t) + \epsilon h^\epsilon(t))g^{-1}(t) = C, \qquad (11)$$

a constant. In the case $\epsilon = 0$, $h(t) = h^p(t) + h^k(t)$ satisfies the equation

$$g(t)h^p(t)g(t)^{-1} = C \qquad (12)$$

where (12) *is the limiting case of equation* (11) *as $\epsilon \to 0$.*

Proof. In the cases $\epsilon \neq 0$, this can be seen by multiplying the equation (11) through by $\frac{1}{\epsilon}$ and differentiating on both sides, making use of equation (6) to note that $\dot{g}(t) = g(t)\, dH$

$$\begin{aligned} \dot{h}^k + \dot{h}^\epsilon &= \left(g(t)^{-1} C\, g(t)\right)^{\cdot}\\ &= -g^{-1}(t)\dot{g}(t)g^{-1}(t)(C)g(t) + g(t)^{-1} C\, \dot{g}(t)\\ &= -g^{-1}(t)(g(t)(\Omega_\epsilon + \Omega_k))g^{-1}(t)(C)g(t)\\ &\quad +g(t)^{-1} C\, (g(t)(\Omega_\epsilon + \Omega_k))\\ &= -(\Omega_\epsilon + \Omega_k)g^{-1}(t)(C)g(t) + g(t)^{-1} C\, (g(t)(\Omega_\epsilon + \Omega_k))\\ &= [h^k, \Omega_\epsilon] + [h^\epsilon, \Omega_\epsilon] + [h^k, \Omega_k] + [h^\epsilon, \Omega_k]\\ \Rightarrow \dot{h}^k &= [h^\epsilon, \Omega_\epsilon] + [h^k, \Omega_k]\\ \dot{h}^\epsilon &= [h^k, \Omega_\epsilon] + [h^\epsilon, \Omega_k] \end{aligned}$$

which is consistent with (7)-(8). Similarly, in the case $\epsilon = 0$, this can be shown by differentiating (12) on both sides

$$\begin{aligned} \dot{h}^p &= \left(g(t)^{-1} C\, g(t)\right)^{\cdot}\\ &= -g^{-1}(t)\dot{g}(t)g^{-1}(t)Cg(t) + g^{-1}(t)C\dot{g}(t)\\ &= -(\Omega_0 + \Omega_k)h^p(t) + h^p(t)(\Omega_0 + \Omega_k)\\ &= [h^p(t), \Omega_0] + [h^p(t), \Omega_k]\\ &= [h^p(t), \Omega_k] \end{aligned}$$

where $\Omega_0 = \begin{bmatrix} 0 & \cdots & \frac{\partial H}{\partial h_1} \\ & & \\ 0 & \cdots & \vdots \\ 0 & \cdots & \frac{\partial H}{\partial h_n} \\ 0 & \cdots & 0 \end{bmatrix}$ and the last line follows since $[\mathfrak{p}, \mathfrak{p}] = 0$ in the case $\epsilon = 0$, and so $[h^p(t), \Omega_0] = 0$. This equation is consistent with equation (10). Taking the limit as $\epsilon \to 0$ in equation (11), note that $\lim_{\epsilon\to 0} \epsilon h^k = 0$, and $\lim_{\epsilon\to 0} \epsilon h^\epsilon = h^p$, and so (11) tends to (12) as $\epsilon \to 0$. □

Proposition 2. *The function*

$$M = h_1^2 + h_2^2 + ... + h_m^2 + \epsilon(h_{m+1}^2 + ... + h_n^2)$$

is a first integral of the system (7)-(8).

Proof. This follows directly from theorem 1: since $g(t)(h^k(t) + h^\epsilon(t))g^{-1}(t) = C$, then

$$\begin{aligned} \kappa(g(t)h(t)^2 g^{-1}(t)) &= \kappa(C^2)\\ \Rightarrow h_1^2(t) + ... + h_m^2(t) + \epsilon(h_{m+1}^2(t) + ... + h_n^2(t)) &= \text{constant} \end{aligned}$$

□

Using the discrete representation

$$g_{i+1} = g_i \exp(\Omega_i h) \qquad (13)$$

where h is a chosen step-size, $t_i = h \cdot i$ and $\Omega_i = \epsilon h^\epsilon(t_i) + h^k(t_i)$, it is possible to construct a, structure-preserving, iterative method

to compute the numerical solution to equations (6)-(8) using equation (11). Firstly, denoting $P(t) = \epsilon h^k(t) + \epsilon h^\epsilon(t)$, then from (11),

$$g(t)P(t)g(t)^{-1} = g(0)P(0)g(0)^{-1},$$

which can be expressed in a discrete form as:

$$P_{i+1} = g_{i+1}^{-1} g_i P_i g_i^{-1} g_{i+1} \tag{14}$$

where from (13), $g_i^{-1} g_{i+1} = \exp(\Omega_i h)$, and so

$$P_{i+1} = \exp(\Omega_i h)^{-1} P_i \exp(\Omega_i h). \tag{15}$$

We then notice that $P_i = \Omega_i^p + \epsilon \Omega_i^k$ by definition, where Ω_i^p stands for the projection on $\mathfrak{p}$ of Ω_i, and Ω_i^k is the projection on $\mathfrak{k}$ (in the 3-D case, for example, $\Omega_i^p = \Omega_i^{13} A_1 + \Omega_i^{23} A_2$ and $\Omega_i^k = \Omega_i^{21} A_3$). Thus, we arrive at the first-order Lie symplectic Euler method

$$\begin{array}{rl} g_{i+1} & = g_i \exp(\Omega_i h) \\ P_{i+1} & = \exp(\Omega_i h)^{-1} P_i \exp(\Omega_i h) \\ \Omega_i & = P_i^p + \frac{1}{\epsilon} P_i^k \end{array} \tag{16}$$

where the initial step values are $\Omega_0 = (\epsilon h^\epsilon)^0 + (h^k)^0$, $P_0 = (\epsilon h^\epsilon)^0 + (\epsilon h^k)^0$ and $g_0 = g(0)$ (where $(h^\epsilon)^0, (h^k)^0$ are the unknowns to be solved for in the shooting method). This is similar to the forward Euler scheme developed in [28] which is developed specifically for the case $\epsilon = 1$. Using such a scheme has an advantage over the popular Runge-Kutta schemes which typically preserve neither the first integrals nor the characteristics of the configuration space; in this case, both are preserved and additionally, as with the method described in [28], it allows one to construct Lie group variational integrators of arbitrarily high order. Also, there is no need for a parametrization of G_ϵ using local coordinates.

A potential drawback of this method is the fact that it cannot be used on the entire system (6) for the case $\epsilon = 0$ due to the degeneracy of Eq. (12). However, if ϵ is chosen to be sufficiently small (e.g. $\epsilon = 1 \times 10^{-10}$in the example on SE(2) in Section 4.3) solutions can be considered near-optimal.

2.2 Matching the boundary conditions of curves satisfying the necessary conditions of optimality

The most obvious way to solve the problem (1)-(2) is to solve the system of equations (6), (21) numerically via a Runge-Kutta scheme, making use of the shooting method to match the boundary conditions in (1) to determine the appropriate initial conditions h^0. This is the method that was first proposed in [3]. The method we develop is similar in that the boundary conditions in (1)-(2) is used directly to set up the shooting function by making use of the "error matrix" $g_{error} = g(t_f, h^0) g_d^{-1}$, and construct the shooting function

$$S(t_f, h^0) = \|\mathrm{Id} - g_{error}\|_1 \tag{17}$$

where $\|\cdot\|_1$ is matrix 1-norm, given for an $n \times m$ matrix by

$$\|A\|_1 = \max_j \left(\sum_{i=1}^{m} |A_{ij}| \right) \quad \text{for} \quad j = 1, 2, ...n.$$

The Lie symplectic Euler scheme (16) is applied to solve for $(g(t), h(t))$ in terms of the initial guess h^0. We then solve for the root h^0 using an iterative Newton's method: set $\Delta_0 = \frac{S(h^0)}{DS(h^0)}$ (where $DS(h^0)$ is the Jacobian of the shooting function (17) which we compute numerically) for the starting guess h^0. The algorithm can be applied iteratively to obtain

$$h_{n+1}^0 = h_n^0 - \frac{S(h_n^0)}{DS(h_n^0)}$$

for $n = 1, 2, 3, ...$ Solving equation (2) in the form of equation (6) ensures R(t) satisfies the orthonormality property for all t, which is not guaranteed when solving numerically by Runge-Kutta schemes.

3 Optimal solutions in the 3-D case

In this section we first solve the extremals in the case where the optimal control problem lifts to a quadratic Hamiltonian. Secondly, we solve the exponential map for the frame bundles of the planar forms where the underlying symmetric space has arbitrary ϵ.

In the 3-D case, the system (1) has the form

$$\begin{cases} \dot{g} & = g(\sum_{i=1}^{j} v_i A_i), \quad 1 < j \leq 3 \\ g(0) & = g_0 \quad \text{and} \quad g(t_f) = g_d. \end{cases} \tag{18}$$

where $A_1, ..., A_3$ are the basis elements

$$A_1 = \begin{bmatrix} 0 & 0 & 1 \\ 0 & 0 & 0 \\ -\epsilon & 0 & 0 \end{bmatrix}, \; A_2 = \begin{bmatrix} 0 & 0 & 0 \\ 0 & 0 & 1 \\ 0 & -\epsilon & 0 \end{bmatrix}, \; A_3 = \begin{bmatrix} 0 & -1 & 0 \\ 1 & 0 & 0 \\ 0 & 0 & 0 \end{bmatrix}, \quad \epsilon \in [-1, 1]. \tag{19}$$

3.1 Solving the extremals in the 3-D case

For the left-invariant control system (18) subject to a cost function of the form (2) yields the optimal Hamiltonian is given by

$$H = \frac{1}{2} \left(\frac{h_1^2}{c_1} + \frac{h_2^2}{c_2} + \frac{h_3^2}{c_3} \right) \tag{20}$$

for $h_i \in \mathfrak{g}_\epsilon$, and so the equations (7) -(8) take the form

$$\begin{cases} \dot{h_1} &= \frac{h_3 h_2}{c_3} - \frac{\epsilon h_3 h_2}{c_2} \\ \dot{h_2} &= \frac{h_1 h_3 \epsilon}{c_1} - \frac{h_1 h_3}{c_3} \\ \dot{h_3} &= \frac{h_1 h_2}{c_2} - \frac{h_1 h_2}{c_1} \end{cases} \tag{21}$$

These equations describe the case $j = 3$ in equation (18): the extremal equations in the cases $j < 3$ can be obtained from (21) by taking any single weight $c_i \to \infty$. Note that no more than one constant weight can tend to infinity at a time or the system may no longer be controllable [23].

It is well-known that the optimal Hamiltonian H is constant along $(g(t), h(t))$. However, from lemma 2, there exists a second constant of motion

$$M = h_1^2 + h_2^2 + \epsilon h_3^2$$

which can be seen to *Poisson-commute* with H, i.e. in the Lie-Poisson bracket,

$$\{H, M\} = 0. \tag{22}$$

The system (21) on $\mathfrak{g}_\epsilon$ in the 3D case is an integrable system [23], and consequently the solution $h(t)$ can be determined analytically. In the general method described in Lawden [29], such a solution may be obtained using the Jacobi elliptic functions $\mathsf{sn}(\cdot, m)$, $\mathsf{cn}(\cdot, m)$ and $\mathsf{dn}(\cdot, m)$:

$$\begin{cases} \mathsf{sn}(x, m) &= \sin(\mathsf{am}(x, m)) \\ \mathsf{cn}(x, m) &= \cos(\mathsf{am}(x, m)) \\ \mathsf{dn}(x, m) &= \sqrt{1 - m^2 \sin(\mathsf{am}(x, m))} \end{cases} \tag{23}$$

where $\mathsf{F}(\cdot, \cdot)$ is the incomplete elliptic integral of the first kind $\mathsf{F}(x, m) = \int_0^x \frac{dt}{1-m^2}$ and $\mathsf{am}(\cdot, m) = \mathsf{F}^{-1}(\cdot, m)$. In Lawden's method, one assumes the general form of the solutions to equations (21) using the Jacobi elliptic functions in terms of the constants h_i^0, H, M and time t.

Denote $\mathsf{sn}(F(t), m)$, $\mathsf{cn}(F(t), m)$, $\mathsf{dn}(F(t), m)$ where $F(t) = \beta t + \gamma$ by $\mathsf{sn}(F(t), m)$, $\mathsf{cn}u$, $\mathsf{dn}u$ respectively. We have the following result

Theorem 2. *The solutions of* (21) *in the cases* $c_3\,\epsilon > c_1 > c_2$, $c_1 > c_2 > \epsilon\, c_3$ *and* $c_2 > c_1 > \epsilon\, c_3$ *have the form*

Case I. $h(t) = (\alpha_1 \mathsf{sn}u, \alpha_2 \mathsf{cn}u, \alpha_3 \mathsf{dn}u)$ $\begin{cases} c_3\,\epsilon > c_1 > c_2 \\ 0 < \frac{(c_1 - c_2)(2H\epsilon c_3 - M)}{(\epsilon c_3 - c_1)(-2Hc_2 + M)} < 1 \end{cases}$	*Case II.* $h(t) = (\alpha_1 \mathsf{sn}u, \alpha_2 \mathsf{dn}u, \alpha_3 \mathsf{cn}u)$ $\begin{cases} c_3\,\epsilon > c_1 > c_2 \\ 0 < \frac{(\epsilon c_3 - c_1)(-2Hc_2 + M)}{(c_1 - c_2)(2\epsilon Hc_3 - M)} < 1 \end{cases}$
Case III. $h(t) = (\alpha_1 \mathsf{cn}u, \alpha_2 \mathsf{sn}u, \alpha_3 \mathsf{dn}u)$ $\begin{cases} c_1 > c_2 > \epsilon\, c_3 \\ 0 < \frac{(c_1 - c_2)(-2H\epsilon c_3 + M)}{(c_2 - \epsilon c_3)(2Hc_1 - M)} < 1 \end{cases}$	*Case IV.* $h(t) = (\alpha_1 \mathsf{dn}u, \alpha_2 \mathsf{sn}u, \alpha_3 \mathsf{cn}u)$ $\begin{cases} c_1 > c_2 > \epsilon\, c_3 \\ 0 < \frac{(c_2 - \epsilon c_3)(2Hc_1 - M)}{(c_1 - c_2)(-2H\epsilon c_3 + M)} < 1 \end{cases}$
Case V. $h(t) = (\alpha_1 \mathsf{sn}u, \alpha_2 \mathsf{cn}u, \alpha_3 \mathsf{dn}u)$ $\begin{cases} c_2 > c_1 > \epsilon\, c_3 \\ 0 < \frac{(c_2 - c_1)(-2H\epsilon c_3 + M)}{(c_1 - \epsilon c_3)(2Hc_2 - M)} < 1 \end{cases}$	*Case VI.* $h(t) = (\alpha_1 \mathsf{sn}u, \alpha_2 \mathsf{dn}u, \alpha_3 \mathsf{cn}u)$ $\begin{cases} c_2 > c_1 > \epsilon\, c_3 \\ 0 < \frac{(c_1 - \epsilon c_3)(2Hc_2 - M)}{(c_2 - c_1)(-2H\epsilon c_3 + M)} < 1. \end{cases}$

(24)

Proof. Here it is shown how $\alpha_i, \beta, m, \gamma$ are obtained for Case I; the method for the other 5 cases is identical. Given the extremal equations (21), in Case I the general form of the solution is:

$$h(t) = (\alpha_1 \mathrm{sn}\,(\beta t + \gamma, m)\,, \alpha_2 \mathrm{cn}\,(\beta t + \gamma, m)\,, \alpha_3 \mathrm{dn}\,(\beta t + \gamma, m)).$$

Differentiating on both sides of this equation and equating the coefficients of $\dot{h}_i(t)$ in this case with the coefficients in (21) gives

$$\left(\frac{1}{c_3} - \frac{\epsilon}{c_2}\right) = \frac{\alpha_1}{\alpha_2 \alpha_3}\beta \tag{25}$$

$$\left(\frac{\epsilon}{c_1} - \frac{1}{c_3}\right) = \frac{-\alpha_2}{\alpha_1 \alpha_3}\beta \tag{26}$$

$$\left(\frac{1}{c_2} - \frac{1}{c_1}\right) = \frac{m^2 \alpha_3}{-\alpha_1 \alpha_2}\beta. \tag{27}$$

Further, the constants of motion

$$H = \frac{1}{2}\left(\frac{\alpha_2^2}{c_2} + \frac{\alpha_3^2}{c_3}\right) \quad \text{and} \quad M = \alpha_2^2 + \epsilon \alpha_3^2$$

along this solution since $\mathrm{sn}(0, m) = 0$, $\mathrm{cn}(0, m) = 1$, $\mathrm{dn}(0, m) = 1$. This is a system of 5 equations in the 5 unknowns α_i, m, β and, solving,

$$\begin{cases} \alpha_1^2 &= \frac{c_1(2H\epsilon c_3 - M)}{\epsilon c_3 - c_1} \\ \alpha_2^2 &= \frac{c_2(2H\epsilon c_3 - M))}{\epsilon c_3 - c_2} \\ \alpha_3^2 &= \frac{c_3(-2Hc_2 + M)}{\epsilon c_3 - c_2} \\ \beta^2 &= \frac{(c_3\epsilon - c_1)(-2Hc_2 + M)}{c_1 c_3 c_2} \\ m^2 &= \frac{(c_1 - c_2)(2H\epsilon c_3 - M)}{(\epsilon c_3 - c_1)(-2Hc_2 + M)} \end{cases} \tag{28}$$

from which we obtain the constraints $\epsilon c_3 > c_1 > c_2$ (so that the solutions are real) and the constraint $0 < \frac{(c_1-c_2)(2H\epsilon c_3 - M)}{(\epsilon c_3 - c_1)(-2Hc_2+M)} < 1$ such that $0 < m < 1$. The value of γ is chosen such that at time $t = 0$, $\mathsf{sn}(\gamma) = \frac{h_1(0)}{\alpha_1}$; thus

$$\gamma = \mathsf{F}\left(\sin^{-1}\left(\frac{h_1(0)}{\alpha_1}\right), m\right).$$

Since $\mathsf{sn}(\beta t + \gamma, m) = h_1(t)/\alpha_1$, then $\mathsf{F}\left(\sin^{-1}\left(\frac{h_1(0)}{\alpha_1}\right), m\right) < \mathsf{F}\left(\frac{\pi}{2}, m\right)$ and it follows that $0 < \mathsf{cn}(\gamma, m) < 1$ (since $\mathsf{cn}(0, m) = 1$ and the first real root of $\mathsf{cn}(\cdot, m)$ is at $\mathsf{cn}(F(\frac{\pi}{2}, m), m) = 0$). The square roots are obtained by noting that since dn is always positive, and $\mathrm{dn}(\beta t + \gamma) = \frac{h_3(t)}{\alpha_3}$, then it follows that $\mathrm{sgn}(\alpha_3) = \mathrm{sgn}(h_3(0))$. Taking $t = 0$, then $h_2(0) = \alpha_2 \,\mathrm{cn}(\gamma, m)$, giving $\mathrm{sgn}(h_2^0) = \mathrm{sgn}(\alpha_2)$. Finally,

$$\begin{aligned} \mathrm{sgn}(\dot{h}_1(0)) &= \mathrm{sgn}(\alpha_1)(\mathrm{sgn}(\mathrm{cn}(\gamma))\mathrm{sgn}(\mathrm{dn}(\gamma))) \\ &= \mathrm{sgn}(\alpha_1) \end{aligned} \tag{29}$$

But, from (21), $\mathrm{sgn}(\dot{h}_1(0)) = \mathrm{sgn}\left(\frac{\epsilon}{c_2} - \frac{1}{c_3}\right)\mathrm{sgn}(h_2^0)\mathrm{sgn}(h_3^0)$. Thus it follows that $\mathrm{sgn}(\alpha_1) = \mathrm{sgn}\left(\frac{\epsilon}{c_2} - \frac{1}{c_3}\right)\mathrm{sgn}(h_2^0)\mathrm{sgn}(h_3^0)$.

In these solutions the constants α_i, β, m are combinations of H, M, h_i^0. In equations (23) there is a constraint on the value m such that $0 < m < 1$. In order to fulfill that constraint in our solution curves $h(t)$, we have the condition on H, M, c_1, c_2, c_3 which is the second condition of each case in table (24). Note that for each ordering of c_i's there are two possible forms of the solution: the two cases together can be seen to represent all possible solutions of the equation (11) for that ordering of c_i's by noting that the constraint on H, M, c_1, c_2, c_3 in the first case is inverted in the second. □

The ordering of the cost values c_i given in this table for each solution will become important when considering the cases $j < 3$ in equation (18) by taking the limit of any single weight $c_i \to \infty$. Clearly if it is required for example that $c_1 \to \infty$ in the case that $c_2 > c_1 > \epsilon c_3$ it would also be required that $c_2 \to \infty$ for the solution to be defined; however, as we have stated, taking more than one weight to infinity may destroy the controllability of the system. Thus it must be ensured that only take the greatest weight in any solution is taken to infinity.

Notice that we have not included all possible orderings in table (24), i.e. for each case where c_i is the greatest weight, the other two weights have a fixed order. Since we can always divide the cost (2) through by c_j ($i \neq j$) to obtain a scalar multiple of the cost $\mathcal{J}$, we can fix the second weight to 1 and set the smallest weight to be in $(0, 1)$; this removes the need to consider both orders of the remaining c_j.

3.2 Matching the boundary conditions in the 3-D case

Here we proceed as in §§2.2 by setting up the shooting function using the error matrix to give a shooting function of the form (17). However, instead of solving the set of equations (6), (21) iteratively, the semi-analytic approach is used where the equations (21) are solved analytically in terms of Jacobi elliptic functions as described in §§3.1 giving a solution $h(t)$ of the form of one of the solutions in table (24) (or the limiting case as $c_i \to 0$ of one of these solutions if $n < 3$ in (1))

The corresponding curve $g(t)$ is then calculated using a generalized Rodrigue's formula, as shown in the following theorem which gives an explicit expression for the matrix exponential on the group for constant time.

Theorem 3. *Given $A \in \mathfrak{g}_\epsilon$ where $\mathfrak{g}_\epsilon$ is the 3D ϵ Lie algebra and $t \in \mathbb{R}$ and $\lambda = \sqrt{\epsilon(a_1^2 + a_2^2) + a_3^2}$, the matrix exponential $g = \exp(At)$ is given by the expression*

$$\exp(At) = \mathsf{Id} + \frac{A}{\lambda}\sin(\lambda t) + \frac{A^2}{\lambda^2}(1 - \cos(\lambda t)) \tag{30}$$

Proof. The exponential series

$$\exp(At) = \mathsf{Id} + At + \frac{(At)^2}{2!} + ... + \frac{(At)^n}{n!} + ... \tag{31}$$

can be simplified as

$$\exp(At) = \sum_{n=0}^{\infty} \frac{t^{2n+1}A^{2n+1}}{(2n+1)!} + \sum_{n=0}^{\infty} \frac{t^{2n}A^{2n}}{(2n)!}. \tag{32}$$

However, in the 3D-case it can be shown that the powers

$$A^{2n+1} = (-1)^{n-1}\lambda^{2n-2}A^2 \tag{33}$$

and

$$A^{2n} = (-1)^n \lambda^{2n} A. \tag{34}$$

Substituting into (32) gives

$$\begin{aligned} \exp(At) &= \sum_{n=0}^{\infty} \frac{t^{2n+1}((-1)^n\lambda^{2n}A)}{(2n+1)!} + \sum_{n=1}^{\infty} \frac{t^{2n+1}(-1)^{n-1}\lambda^{2n-2}A^2}{(2n)!} \\ &= \frac{A}{\lambda}\sum_{n=0}^{\infty} \frac{(\lambda t)^{2n+1}(-1)^n}{(2n+1)!} + \mathsf{Id} \\ &\quad + \frac{A^2}{\lambda^2}\sum_{n=1}^{\infty}(\frac{t^{2n+1})(-1)^{n-1}\lambda^{2n-2}A^2}{(2n)!} \\ &= \frac{A}{\lambda}\sum_{n=0}^{\infty} \frac{(\lambda t)^{2n+1}(-1)^n}{(2n+1)!} + \mathsf{Id} + \frac{A^2}{\lambda^2}\sum_{n=0}^{\infty} \frac{(t\lambda)^{2n}(-1)^n}{(2n)!} + \frac{A^2}{\lambda^2} \\ &= \frac{A}{\lambda}\sin(\lambda t) + \mathsf{Id} + \frac{A^2}{\lambda^2}(1 - \cos(\lambda t)). \end{aligned}$$

. □

The curve $g(t)$ can then be solved for using the iterative expression $g_{i+1} = g_i \exp(A_i h)$ as in equation (16). In order to match the boundary conditions, we solve for the root of the shooting function using the iterative Newton's method as in §§2.2.

3.3 Dynamic feasibility

In our computations the time domain is scaled with respect to true final time so that time remains in the interval $[0, 1]$. This scaled time is denoted by t to differentiate it from the real time τ. In general, it may be assumed that τ is related to t by an equation $t = f(\tau)$. Thus

$$\frac{d}{d\tau} = \frac{df(\tau)}{d\tau}\frac{d}{dt}. \tag{35}$$

In this way, from equation (1),

$$\frac{d}{d\tau}v_i(f(\tau)) = \frac{df(\tau)}{d\tau}F(v_i) + \frac{df(\tau)}{d\tau}u_i \tag{36}$$

and correspondingly the acceleration u_i in terms of real time is

$$u_i(\tau) = \frac{dv_i(f(\tau))}{d\tau}\Big/\frac{df(\tau)}{d\tau} - F(v_i(f(\tau))). \tag{37}$$

In our particular case we will assume that $t = \frac{\tau}{T_f}$. Thus the optimal velocities v_i and their corresponding accelerations u_i (given in equation (1)) are a functions of τ and T_f. In this way, manoeuvre duration affects the acceleration profile. Thus when considering dynamic feasibility, a criterion for choosing T_f such that the calculated maximum acceleration is less than or equal to the actuator's limit $u_{\max}$ can be determined. Making use of the same motion control profile but by using unscaled time τ allows us to reduce the magnitude to within the feasible level $\|u\| < u_{\max}$ by choosing a suitably large transfer time T_f. This method is used in sections 4.2.1, 4.3.2 to determine feasible torque and thrust values in optimal motion planning examples.

4 Examples

In this section, two of the problems considered in references ([1, 2], [4], [8–10]) are used to illustrate the applications of our method. We chose to focus on the case $n < 3$ and consider the cases $(\epsilon = 1, i = 1, 2)$ and the limiting case $\epsilon \to 0$ in $(\epsilon = 0, i = 1, 3)$.

4.1 Orientation of an underactuated spacecraft with reaction wheels

In [5], the dynamic equations of motion of a spacecraft with reaction wheels without external disturbances is given by

$$J\dot{\boldsymbol{\omega}} = -\boldsymbol{\omega} \times (J\boldsymbol{\omega} + \mathbf{L}) - \dot{\mathbf{L}} \tag{38}$$

where $\boldsymbol{\omega} = [\omega_1, \omega_2, \omega_3]^\top$ is the angular velocity vector of the spacecraft in body fixed co-ordinates, J is the inertia tensor and $\mathbf{L}$ the angular momentum of the reaction wheels. This equation can be expressed on the directed cosine matrix $g(t) \in \mathsf{SO}(3)$, the Special Orthogonal Group, where the column vectors of the matrix define an orthonormal frame fixed to the body. Thus the kinematics are described by a differential equation of the form (1) for $\alpha_i = 0, \epsilon = 1, n = 3$.

In control of underactuated spacecraft, $n < 3$ so that the degrees of freedom of the dynamical system are higher than number of actuators. Developing motion planning laws for such systems allows fully actuated systems to be operated as underactuated, for example re-pointing a spacecraft in the case of an actuator failure [19] or to conserve propellant in some manoeuvres [14]. Also systems that are underactuated by design have the advantage over fully actuated systems of being easier to design and cheaper to build; therefore with the current move toward smaller, cheaper spacecraft, underactuated control presents an advantage.

Assuming without loss of generality that there are just two reaction wheels along the X and Y axes such that $\mathbf{L} = [L_1, L_2, 0]^\top$ then the spacecraft is controllable by the two wheels if and only if the total angular momentum is zero

$$J\boldsymbol{\omega} + \mathbf{L} = 0 \quad \Leftrightarrow \quad J\dot{\boldsymbol{\omega}} = -\dot{\mathbf{L}}. \tag{39}$$

Thus from here on it is assumed that $\boldsymbol{\omega} = [\omega_1, \omega_2, 0]^\top$. Expressing the attitude kinematics of the spacecraft $g(t) \in \mathsf{SO}(3)$, in this case (where J is defined relative to the center of mass aligned with the principal axes)

$$\dot{g}(t) = -g(t)\left(\frac{L_1}{I_1}A_1 + \frac{L_2}{I_2}A_2\right) \tag{40}$$

where A_1, A_2 are given by (19) at $\epsilon = 1$, and I_i are the principle moments of inertia of the satellite. The aim of the underactuated re-pointing problem is to determine the angular velocities L_i required to re-point a spacecraft from its initial position $g(0) = g_0$ to a prescribed final position $g(t_f) = g_d$ while minimizing the cost function:

$$\mathcal{J} = \frac{1}{2}\int_0^{t_f} c_1\omega_1^2 + c_2\omega_2^2 \; dt \tag{41}$$

where $c_1, c_2 > 0$ are constant weights. Varying the weights c_i allows us to produce perturbations of the curves between g_0 and g_d which can be used for avoidance of certain spacecraft orientations. We choose to focus on the case $c_1 = 1, c_2 = 0.25$; in particular, we consider the optimal control problem

$$\begin{cases} g_0 &= \mathrm{Id} \\ g_d &= \exp(-0.897 A_2)\exp(-\frac{\pi}{2}A_3) \\ t_0 &= 0,\ t_f = 1 \\ c_2 &= 0.25,\ c_1 = 1,\ c_3 \to \infty \end{cases} \tag{42}$$

4.1.1 Calculating the extremals

In the case of problem (42), the solution takes the form

$$\begin{aligned} & (h_1(t), h_2(t), h_3(t)) \\ = \ & (\alpha_1 \mathsf{sn}(F(t), m), \alpha_2 \mathsf{cn}(F(t), m), \alpha_3 \mathsf{dn}(F(t), m)) \end{aligned} \tag{43}$$

in table (24), for which the coefficients are the limiting case as $c_3 \to \infty$ of the coefficients α_i, β, m:

$$\begin{cases} \alpha_1 = \mathrm{sgn}\left(h_2^0 \cdot h_3^0 \cdot \left(\frac{-\epsilon}{c_2}\right)\right)\sqrt{2Hc_1} \\ \alpha_2 = \mathrm{sgn}(h_2^0)\sqrt{2Hc_2} \\ \alpha_3 = \mathrm{sgn}(h_3^0)\sqrt{\frac{(M-2Hc_2)}{\epsilon}} \end{cases} \quad \begin{cases} \beta = \sqrt{\frac{\epsilon(M-2Hc_2)}{c_1 c_2}} \\ m = \sqrt{\frac{(2H(c_1-c_2))}{M-2Hc_2}} \\ \gamma = \mathsf{F}(\sin^{-1}\left(\frac{h_1^0}{\alpha_1}\right), m). \end{cases} \tag{44}$$

When determining the extremal curves for this particular problem by minimizing the function (17) the solution $g(t)$ that initially obtained has many fluctuations and does not approach the final condition directly ; the projection of this curve on the first column of $g(t)$ is shown in Fig. 1. a. While this is a solution, it is clearly not minimizing. In order to determine the a lower-cost solution, we solved for the h^0 which minimized the function (49), using the method described in section 4.2. The projection on the first column of the curve $g(t)$ obtained using this method is shown in Fig. 1.b. The α_i, β, γ values obtained for this curve are used in the computations.

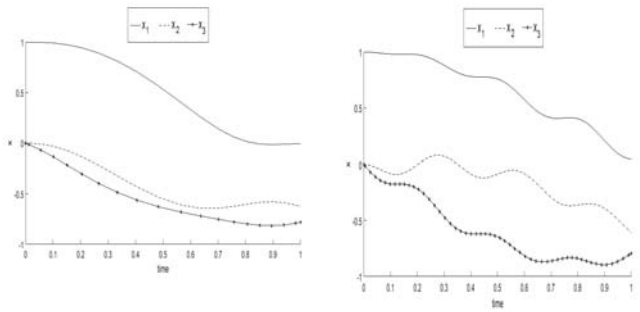

$(a.)$ $(b.)$

Figure 1: Projection on the first column of $g(t)$, $x = g(t)\cdot[1,0,0]^\top$ a.) Optimizing extremal; b.) Solution curve satisfying the necessary and boundary conditions

$$\begin{cases} \alpha_1 &= 2.387 \\ \alpha_2 &= 1.193 \\ \alpha_3 &= -2.301 \end{cases} \quad \begin{cases} \beta &= 4.601 \\ m &= 0.807 \\ \gamma &= 0.434. \end{cases} \tag{45}$$

Substituting into the equations $\omega_i = \frac{h_i}{c_i}$, the angular velocities are obtained

$$\omega_1 = 2.387\,\mathsf{sn}(4.601\,t + 0.434, 0.807)\ \mathrm{rad}\cdot s^{-1} \tag{46}$$

$$\omega_2 = 4.77\,\mathsf{cn}(4.601\,t + 0.434, 0.807)\ \mathrm{rad}\cdot s^{-1} \tag{47}$$

$$\omega_3 = 0. \tag{48}$$

4.2 Optimal motions of minimum energy type

The method described in the previous sub-section is used to determine the extremals of the optimal control problem (1)-(2). However, there may be several possible extremals for this problem, since in the Pontryagin's principle extremality is only a necessary condition for optimality, and a method is require to select the cost-minimizing extremal (this is illustrated in Fig. 1 for a particular example).

To implement this using parameter optimization, a new function is constructed which is used to select the extremal which additionally minimizes the quadratic performance metric $\mathcal{J}$ in equation (2). Although the expressions of v_1, v_2 and v_3 are analytic, and so the function $\mathcal{J}$ can be determined analytically in each case, we use the function trapz of matlab which performs numerical integration of time-dependent vectors via the trapezoidal method. This method approximates the integration over an interval by breaking the area down into trapezoids with more easily computable areas. This gives rise to the function

$$\mathcal{J} = \frac{t_f}{2N}\sum_{n=1}^{N}\Big(\sum_{i=1}^{3} c_i (v_i(t_n)^2 - v_i(t_{n+1})^2)\Big). \tag{49}$$

where $N+1$ is the number of evenly-spaced points in the integrand $v(t)$. We seek the minimum of the function

$$y(h^0, t_f) = \|\mathrm{Id} - g_{error}\|_1 + w\,\mathcal{J} \tag{50}$$

using the matlab function fminunc. The weight w in (50) must be fixed, since determining the minimum of (50) so that the boundary conditions are still met is a multi-objective problem requiring to minimize both the condition (17) and the performance metric value (49). In practice, it serves us best to minimize $y(h^0, t_f)$ for some low value of w to obtain an h^0 value for which cost is minimized, and then to decrease w incrementally to the case $w = 0$ to obtain the h^0 which initializes the low-cost extremal.

4.2.1 Dynamically feasible curves

Using the condition $\omega_3 = 0$ required from the zero-angular momentum condition, and substituting into equation (39) gives

$$u_1 = \dot{\omega}_1 I_1 \quad (51)$$
$$u_2 = \dot{\omega}_2 I_2 \quad (52)$$

Substituting the right hand side of equation (43) into (72)-(73) gives the torques (in the case of scaled time):

$$u_1 = \frac{I_1\,\alpha_1\,\beta}{c_1}\,\mathsf{dn}(\beta t+\gamma,m)\,\mathsf{cn}(\beta t+\gamma,m)\;N\cdot m \quad (53)$$
$$u_2 = -\frac{I_2\,\alpha_2\,\beta}{c_2}\,\mathsf{dn}(\beta t+\gamma,m)\,\mathsf{sn}(\beta t+\gamma,m)\;N\cdot m. \quad (54)$$

Substituting in the values for $\alpha_1, \alpha_2, \beta$ and m and the inertia values I_1 and I_2 for a typical cubesat ($I_1 = 0.141728kg\cdot m^2, I_2 = 0.153784\ kg\cdot m^2, I_3 = 0.079546\ kg\cdot m^2$) gives the torques

$$\begin{aligned} u_1 &= 1.556\,\mathsf{cn}(4.601\,t+0.434,0.807)\cdot \\ &\quad\ \mathsf{dn}(4.601\,t+0.434,0.807)\;N\cdot m \\ u_2 &= -3.378\,\mathsf{sn}(4.601\,t+0.434,0.807)\cdot \\ &\quad\ \mathsf{dn}(4.601\,t+0.434,0.807)\;N\cdot m. \end{aligned}$$

Choosing the reaction wheel torque of $10mNm$, it is clear that the torques obtained lie outside of this feasible value. In order to address the problem of dynamic feasibility we then convert the problem on $t\in[0,1]$ to one on $\tau\in[0,T_f]$. On this time interval, using equation (35), the torques take the form

$$u_i(\tau,T_f) = \frac{-I_i}{T_f^2}\dot{\omega}\left(\frac{\tau}{T_f}\right). \quad (55)$$

Using equation (55), the torques u_1 and u_2 are related to the final true time T_f through the equations

$$u_1(\tau,T_f) = -\frac{\alpha_1\,\beta}{c_1}\,\frac{I_1}{T_f^2}\,\mathsf{cn}(\frac{\beta\tau}{T_f}+\gamma,m)\,\mathsf{dn}(\frac{\beta\tau}{T_f}+\gamma,m)\;N\cdot m \quad (56)$$
$$u_2(\tau,T_f) = \frac{\beta\,\alpha_2}{c_2}\,\frac{I_2}{T_f^2}\,\mathsf{sn}(\frac{\beta\tau}{T_f}+\gamma,m)\,\mathsf{dn}(\frac{\beta\tau}{T_f}+\gamma,m)\;N\cdot m, \quad (57)$$

which gives us a lower bound for total transfer time,

$$\frac{I_i\alpha_i\beta}{\max(u_i)c_i} \le T_f^2. \quad (58)$$

Substituting our maximum reaction wheel torque value $u_{max} = 10\times mNm$ into equation (58) allows us to pick a feasible time T_f, which will bring our torque values in equation (55) back into alignment with feasible reaction wheel values. For the torque u_1 the lower bound is $12.476s$, and for the torque u_2, the lower bound is $18.378s$. Thus, substituting $T_f = 20s$ into equations (75)-(76) gives feasible torques $u_i(\tau), i = 1,2$ developing in real time which can be used to carry out the manoeuvre optimally with torque magnitudes below the practical constraints.

4.3 Planar spacecraft optimal docking problem with velocity constraints

Rendezvous and docking manoeuvres between an active spacecraft and a passive target are of importance to space station applications. For a realistic spacecraft docking manoeuvre, the approach direction is constrained along a target docking axis (as in Fig. 2) and the approach must be carried out in an optimal way.
Consider an active spacecraft traveling in the $e_1 - e_2$ plane driven by thrusters located at either end of one axis of the spacecraft and able to rotate at an angular velocity ω about the e_3 axis due to torque provided by a reaction wheel, and equipped with a brake. The dynamic equations of motion of such a spacecraft without external disturbances are given by [9]

$$\begin{aligned} \dot{x} &= v\cos(\theta) \\ \dot{y} &= v\sin(\theta) \\ \dot{\theta} &= \omega \\ u_v &= W\dot{v} \quad (59) \\ u_\omega &= \dot{\omega} I_3 \quad (60) \end{aligned}$$

where v is translational velocity, u_v is the thruster force, W is the mass of the active spacecraft and u_ω is the torque of the reaction wheel. This problem is equivalent to the Reeds-Shepp framing of the problem of Dubins. Dubins showed in [9], using geometrical arguments that any such path will consist of maximum curvature and/or straight line segments. The same result was later shown using Pontryagin's maximum principle [30]. Here we demonstrate the simple semi-analytical method to compute the optimal path.

The configuration space of the active spacecraft can be described by a curve $g(t)\in\mathsf{SE}(2)$, the 3D Special Euclidean Group, and expressed in matrix form as:

$$g(t) = \begin{bmatrix} \cos\theta & -\sin\theta & x \\ \sin\theta & \cos\theta & y \\ 0 & 0 & 1 \end{bmatrix}. \quad (61)$$

The assumption that the spacecraft can move backward or forwards at a controlled velocity v is a sliding constraint:

$$\begin{bmatrix} \dot{x} \\ \dot{y} \end{bmatrix} = \begin{bmatrix} \cos\theta & -\sin\theta \\ \sin\theta & \cos\theta \end{bmatrix}\begin{bmatrix} v \\ 0 \end{bmatrix}. \quad (62)$$

Differentiating equation (61) and taking into the account the constraint (62) it is easily shown that the non-holonomic kinematic constraint can be expressed as a left-invariant differential equation:

$$\dot{g} = g(t)\begin{bmatrix} 0 & -\omega & v \\ \omega & 0 & 0 \\ 0 & 0 & 0 \end{bmatrix}. \quad (63)$$

In terms of the basis A_1, A_2, A_3 in (19) at $\epsilon = 0$, this is the equation

$$\dot{g}(t) = g(t)\,(vA_1 + \omega A_3) \tag{64}$$

i.e. the control system is of the form (1) with $\epsilon = 0, i = 1, 3$. The performance metric is:

$$\mathcal{J} = \frac{1}{2}\int_0^{t_f} c_1 v^2 + c_3\omega^2 dt \tag{65}$$

where $c_i > 0$, $i = 1, 3$ are constant weights. Varying the weights c_i allows us to produce perturbations of the curves between g_0 and g_d for obstacle avoidance. We choose the weighs $c_3 = 1$, $c_1 = 0.2$.

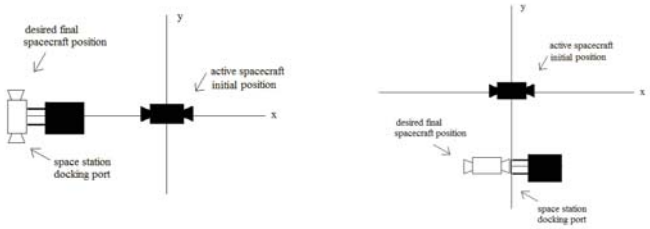

a) b)

Figure 2: a.) The active/passive spacecraft configuration used in problem (66) b.) Configuration of active and passive spacecraft used in the computations for Fig. 3 c.) and 3 d.)

As in the Fig. (2.b), we choose the active spacecraft initial position at the origin $[0, 0]$, and the initial direction to be $\theta(0) = 0$. The final desired orientation is the angle $\theta(t_f) = \frac{\pi}{2}$ at which orientation the satellite is positioned at $[0, -1]$. Accordingly, the following parameters are used:

$$\begin{cases} g_0 &= \mathrm{Id} \\ g_d &= \exp(-A_2)\exp(A_3\frac{\pi}{2}) \\ t_0 &= 0,\ t_f = 1 \\ c_1 &= 0.2,\ c_3 = 1. \end{cases} \tag{66}$$

4.3.1 Calculating the optimal extremal

For the problem (66), the form of solution $h(t)$ is

$$\begin{aligned} & (h_1(t), h_2(t), h_3(t)) \\ = \ & (\alpha_1 \mathsf{sn}(F(t), m), \alpha_2 \mathsf{cn}(F(t), m), \alpha_3 \mathsf{dn}(F(t), m)) \end{aligned} \tag{67}$$

in table (24), where the coefficients are the limiting case as $c_2 \to \infty$ of the coefficients α_i, β, m, to give

$$\begin{cases} \alpha_1 &= \mathrm{sgn}(h_2^0 \cdot h_3^0 \cdot \frac{c_2 - \epsilon c_3}{c_2 c_3})\sqrt{\frac{c_1(M - 2Hc_3\epsilon)}{c_1 - c_3\epsilon}} \\ \alpha_2 &= \mathrm{sgn}(h_2^0)\sqrt{M - 2Hc_3\epsilon} \\ \alpha_3 &= \mathrm{sgn}(h_3^0)\sqrt{2Hc_3} \\ \beta &= \frac{2H(c_1 - c_3\epsilon)}{c_1 c_3} \\ m &= \sqrt{\frac{(M - 2Hc_3\epsilon)}{2H(c_1 - c_3\epsilon)}} \\ \gamma &= \mathsf{F}(\sin^{-1}\left(\frac{h_1^0}{\alpha_1}\right), m) \end{cases} \tag{68}$$

By finding h^0 such that the function (49) is minimized for $w = 1 \times 10^{-5}$ and making use of method described in section 4.2 to obtain a low-cost solution, the initialization $h^0 = \begin{bmatrix} 0.387 & -0.594 & 1.558 \end{bmatrix}$ is obtained. Fig. 3 shows the motion of an $x - y$-frame attached to the spacecraft at the initial position $(1, 0)$, $(0, 1)$ to show the evolution of the frame to the final position given by (66); the result for this transfer is shown in Fig. 3.a); the motion of the body frame for three other possible similar transfers as computed by using this method are shown in 3.b) to 3.d).

The numerical values of the coefficients $\alpha_i, \beta, m, \gamma$ in equations (67) are given by

$$\begin{cases} \alpha_1 &= -0.709 \\ \alpha_2 &= -0.709 \\ \alpha_3 &= 1.782 \end{cases} \quad \begin{cases} \beta &= 1.782 \\ m &= 0.890 \\ \gamma &= -0.609 \end{cases} \tag{69}$$

giving rise to the angular velocity ω and linear velocity v,

$$v = -3.547\,\mathsf{sn}(1.782\,t - 0.609, 0.890)\ m \cdot s^{-1} \tag{70}$$

$$\omega = 1.782\,\mathsf{dn}(1.782\,t - 0.609, 0.890)\ rad \cdot s^{-1}. \tag{71}$$

4.3.2 Feasible curves

From (59)-(60), the torque of the reaction wheel u_ω and the thruster force u_v (in the case of scaled time) are

$$u_v(t) = \frac{\alpha_1\,\beta W}{c_1}\,\mathsf{dn}(\beta t + \gamma, m)\,\mathsf{cn}(\beta t + \gamma, m)\ N \tag{72}$$

$$u_\omega(t) = -\frac{I_3\,\alpha_3\,\beta m^2}{c_3}\,\mathsf{sn}(\beta t + \gamma, m)\,\mathsf{cn}(\beta t + \gamma, m)\ N \cdot m \tag{73}$$

As in section 4.2.1, substituting in the values for $\alpha_1, \alpha_2, \beta$ and m and the inertia values I_1 and I_2 for the typical cubesat used in section 4.2.1 into (73) gives

$$\begin{aligned} u_\omega(t) = \ & -0.200\,\mathsf{sn}(1.782\,t - 0.609, 0.890) \cdot \\ & \mathsf{cn}(1.782\,t - 0.609, 0.890)\ N \cdot m \end{aligned}$$

for which the magnitude lies outside of the maximum feasible reaction wheel torque of $10 \times 10^{-3} N \cdot m$.

Furthermore, substituting in the feasible cubesat mass $10kg$ into equation (72) gives rise to

$$u_v(t) = -63.213\ \mathsf{cn}(1.782\,t - 0.609, 0.890) \cdot \mathsf{dn}(1.782\,t - 0.609, 0.890)\ N.$$

Since the thrust magnitude for cubesat actuators is typically of the order of $10^{-4}N$, this thrust is not feasible.

From equation (55) the relation of the final "true" time T_f to t gives lower bounds on the total transfer time,

$$\begin{cases} \frac{W\alpha_1\beta}{\max(u_1)c_1} & \leq T_f^2 \\ \frac{I_3 m^2 \alpha_3 \beta}{\max(u_3)c_3} & \leq T_f^2. \end{cases} \tag{74}$$

Substituting in our max torque value $\max(u_3) = 10mNm$ gives a lower bound of 4.474. However, the lower bound on T_f arising from the maximum thrust force $\max(u_1) = 6.5 \times 10^{-4}N$ is 311.850. Thus, clearly the manoeuvre is made in a cost-minimizing way with feasible thrust values by using the equations in true time

$$u_v(\tau) = -\frac{\alpha_1\,\beta}{c_1}\,\frac{W}{T_f^2}\,\mathsf{cn}(\frac{\beta\tau}{T_f} + \gamma, m)\,\mathsf{dn}(\frac{\beta\tau}{T_f} + \gamma, m) \tag{75}$$

$$u_\omega(\tau) = \frac{\beta\,\alpha_3}{c_3}\,\frac{I_3}{T_f^2}\,\mathsf{sn}(\frac{\beta\tau}{T_f} + \gamma, m)\,\mathsf{cn}(\frac{\beta\tau}{T_f} + \gamma, m), \tag{76}$$

where $T_f = 320s$, the numerical values of α_i, β, γ are given in (69) and the c_i-values in (66).

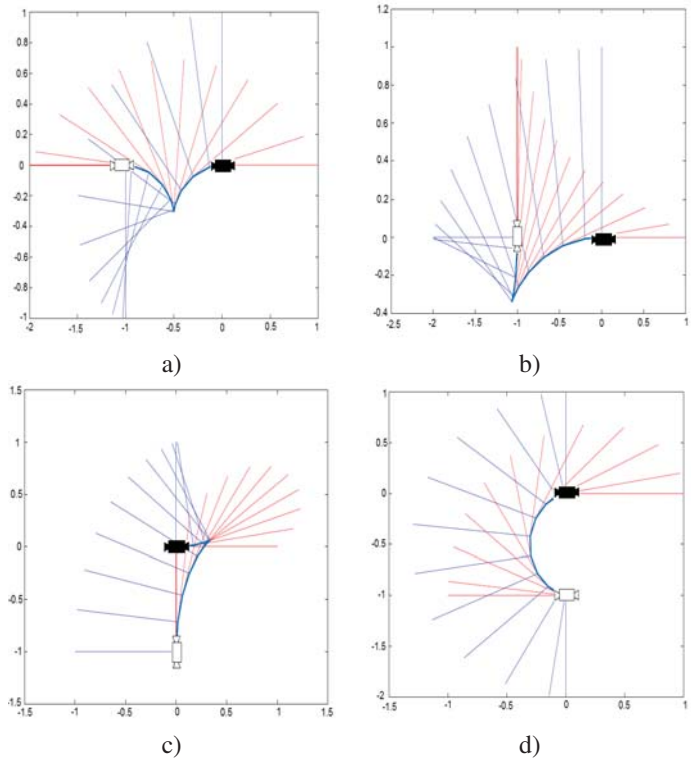

Figure 3: Motion of the x-y-frame attached to the spacecraft during the transfer: a)-b) with the configuration in Fig. 2 b.) and c)-d) with the configuration in Fig 2 a.)

5 Conclusion

The proposed method provides a motion planning algorithm for a class of mechanical control systems that does not require parameterization of the systems configuration space. New techniques for solving a boundary value problem that arises from the application of Pontryagin's maximum principle to a class of optimal control problems on 3-D Lie groups is presented. While prior work has concentrated either on numerical shooting or using an extended system or continuation methods for systems with kinematics defined on the frame bundles of spaces with a particular curvature, our method is applicable to frame bundles for spaces of arbitrary constant curvature and in n dimensions. In the 3-D case, the method reduces the boundary value problem to a semi-analytic shooting method by exploiting the analytic solution to the extremal equations. The method reduces the number of equations to be integrated compared to the fully numerical shooting method. In addition, since the optimal velocities and corresponding control

accelerations for this class of problems can be expressed in terms of Jacobi elliptic functions, the dynamic constraints can be satisfied along the derived curve by reparametrizing time. While we cannot claim rigorously that the resulting motion satisfies the sufficient conditions for optimality, we provide a numerical scheme which chooses the most optimal curve amongst the curves computed that satisfy the necessary and boundary conditions. The approach could be equally applicable to problems in robotics that evolve on the 6-D group $\mathsf{SE}(3)$.

References

[1] Biggs, J. D., & L. Colley (2016). Geometric attitude motion planning for spacecraft with pointing and actuator constraints. *Journal of Guidance, Control and Dynamics*, *39(7)*, 1672-1677.

[2] Maclean, C., D. Pagnozzi, & J. D. Biggs (2014). Planning natural repointing manoeuvres for nano-spacecraft. *IEEE Transactions on Aerospace and Electronic Systems*, *50(3)*, 2129-2145.

[3] Spindler, K. (1996). Optimal attitude control of a rigid body. *Applied Mathematics & Optimization*, *34(1)*, 79-90.

[4] Biggs, J. and N. Horri (2012). Optimal geometric motion planning for a spin-stabilized spacecraft. *Systems and Control Letters*, 61(4), 609-616.

[5] Biggs, J. D., Y. Bai and H. C. Henninger(2017). Attitude guidance and tracking for spacecraft with two reaction wheels. *International Journal of Control*, *accepted February 2017*. doi/full/10.1080/00207179.2017.1299944

[6] Spindler, K (1999). Attitude control of underactuated spacecraft. *IEEE 1999 European Control Conference*, Karlsruhe, Germany.

[7] Biggs, J. D., and Holderbaum, W.(2009) Optimal kinematic control of an autonomous underwater vehicle. *IEEE Transactions on Automatic Control*, *54 (7)*, 1623-1626.

[8] Bretl, T. and Z. McCarthy (2014). Quasi-static manipulation of a Kirchhoff elastic rod based on a geometric analysis of equilibrium configurations. *International Journal of Robotics Research*, *33(1)*, 48-68.

[9] Dubins, L. E. (1957). On curves of minimal length with a constraint on average curvature, and with prescribed initial and terminal positions and tangents. *American Journal of Mathematics*, *79*, 497-516.

[10] Liu, Y. and Z. Geng (2014). Finite-time optimal formation tracking control of vehicles in horizontal plane. *Nonlinear Dynamics*, *76(1)*, 481-495.

[11] Biggs, J. D., W.Holderbaum, & V. Jurdjevic (2007). Singularities of optimal control problems on some 6-D Lie groups. *IEEE Transactions on Automatic control*, *52(6)*, 1027-1038

[12] Mukherjee, R., B. R. Emond, & J. L. Junkins (1997). Optimal trajectory planning for mobile robots using Jacobian elliptic functions. *International Journal of Robotics Research*, *16(6)*, 826-839.

[13] Murray, R. M. and S. S. Sastry (1993). Nonholonomic motion planning: Steering using sinusoids. *IEEE Transactions on Automatic Control*, *38(5)*, 700-716.

[14] Coverstone-Carroll, V. (1996). Detumbling and reorienting underactuated rigid spacecraft. *Journal of Guidance, Control and Dynamics*, *19(3)*, 708-710.

[15] Leonard, N. E. and P. S. Krishnaprasad (1994). Control of switched electrical networks using averaging on Lie groups. *Proceedings of 33rd IEEE Conference on Decision and Control*, Orland, FL, USA, 1919-1924.

[16] D'Allessandro, D (1993). *Introduction to quantum control and dynamics*. Boca Raton, FL: CRC Press

[17] Patil, S., J. Pan, P. Abbeel, & K. Goldberg. (2015). Planning curvature and torsion constrained ribbons in 3d with application to intracavitary brachytherapy. *IEEE Transactions on Automation Science and Engineering*, *12(4)*, 1332-1345.

[18] Brockett, R. W. and L. Dai (1991). Non-holonomic kinematics and the role of elliptic functions in constructive controllability. *IEEE R&A Workshop on Nonholonomic Motion Planning*, Sacremento, CA, 1-17.

[19] Leonard, N. E. and P. S. Krishnaprasad (1995). Motion control of drift-free, left-invariant systems on Lie groups. *IEEE Transactions on Automatic Control*, *40(9)*, 1539-1554.

[20] Chitour, Y. (2002). Path planning on compact Lie groups using a homotopy method. *Systems and Control Letters*, *47(5)*, 383-391.

[21] Lafferriere, G. and H. Sussmann (1991). Motion planning for controllable systems without drift. *Proceedings of the IEEE International Conference on Robotics and Automation* Sacramento, CA, USA.

[22] Jurdjevic, V. and H. J. Sussmann (1972). Control systems on Lie groups. *Journal of Differential Equations*, *12*, 313-329.

[23] Jurdjevic, V. (1997). *Geometric Control Theory*, UK: Cambridge University press.

[24] Jurdjevic, V. (2001). Hamiltonian point of view of non-Euclidean geometry and elliptic functions. *Systems and Control Letters*. *43*, 25-41.

[25] Judjevic, V.(2005). Integrable Hamiltonian systems on complex Lie groups. *Memoirs of the American Mathematical Society*, *178*, 20-25.

[26] Boltyanskii, V., R. Grigor'evich, V. Gamkrelidze, and L. S. Pontryagin (1960). *The theory of optimal processes: I. The maximum principle*. TRW Space Technology Labs, Los Angeles, California.

[27] Lawden, J. (2013). *Elliptic functions and their applications Vol. 80*, Berlin, Springer Science & Business Media.

[28] Bloch, A. M., I. I. Hussein, M. Leok and A. K. Sanyal (2009). Geometric structure-preserving optimal control of a rigid body. *Journal of Dynamical and Control Systems*, *15*(3), 307-330.

[29] Lawden, D. F. (2013). *Elliptic functions and applications*. Berlin: Springer Science & Business Media.

[30] Boissonnat, J-D., A. Cérézo, and J. Leblond (1992). Shortest paths of bounded curvature in the plane. *Proceedings of the IEEE International Conference on Robotics and Automation*, Nice, France.

[31] Bloch, A. M., J. Baillieul, P. E. Crouch, J. E. Marsden, D. Zenkov, P. S. Krishnaprasad, and R. M. Murray (2003). *Nonholonomic mechanics and control Vol. 24* New York: Springer.

[32] Bloch, A.M., P. E. Crouch and T. S. Ratiu (1994). *Sub-Riemannian optimal control problems*. In: Field's Institute Communiations Vol. 3. Providence, Rhode Island: American Mathematical Society, 35-48

[33] Baillieul, J. (1975). *Some optimization problems in geometric control theory*. Ph.D. thesis, Harvard University, USA.

[34] Brockett, R. W. (1973). *Lie algebras and Lie groups in control theory*. In: Geometric methods in system theory. Netherlands:Springer, 43-82.